Bioorganic Chemistry 150 (2024) 107555

Contents lists available at ScienceDirect

Bioorganic Chemistry

journal homepage: www.elsevier.com/locate/bioorg

sp^2-Iminosugar azobenzene *O*-glycosides: Light-sensitive glycosidase inhibitors with unprecedented tunability and switching factors

Gonzalo Rivero-Barbarroja [a], M. Carmen Padilla-Pérez [a], Stéphane Maisonneuve [b], M. Isabel García-Moreno [a], Ben Tiet [c], David J. Vocadlo [c,d], Juan Xie [b,*], José M. García Fernández [e,*], Carmen Ortiz Mellet [a,*]

[a] Department of Organic Chemistry, Faculty of Chemistry, University of Seville, c/ Profesor García González 1, 41012 Sevilla, Spain
[b] ENS Paris-Saclay, CNRS, Photophysique et Photochimie Supramoléculaires et Macromoléculaires, Université Paris-Saclay, Gif-sur-Yvette 91190, France
[c] Department of Chemistry, Simon Fraser University, Burnaby, British Columbia, V5A 1S6, Canada
[d] Department of Molecular Biology and Biochemistry, Simon Fraser University, Burnaby, British Columbia, V5A 1S6, Canada
[e] Instituto de Investigaciones Químicas (IIQ), CSIC – Universidad de Sevilla, Américo Vespucio 49, 41092 Sevilla, Spain

ARTICLE INFO

Keywords:
Azobenzene
β-glucocerebrosidase
Glycosidase inhibitors
sp^2-Iminosugars
Photoswitchers

ABSTRACT

The conventional approach to developing light-sensitive glycosidase activity regulators, involving the combination of a glycomimetic moiety and a photoactive azobenzene module, results in conjugates with differences in glycosidase inhibitory activity between the interchangeable *E* and *Z*-isomers at the azo group that are generally below one-order of magnitude. In this study, we have exploited the chemical mimic character of sp^2-iminosugars to access photoswitchable *p*- and *o*-azobenzene α-*O*-glycosides based on the *gluco*-configured representative ONJ. Notably, we achieved remarkably high switching factors for glycosidase inhibition, favoring either the *E*- or *Z*-isomer depending on the aglycone structure. Our data also indicate a correlation between the isomeric state of the azobenzene module and the selectivity towards α- and β-glucosidase isoenzymes. The most effective derivative reached over a 10^3-fold higher inhibitory potency towards human β-glucocerebrosidase in the *Z* as compared with the *E* isomeric form. This sharp contrast is compatible with ex-vivo activation and programmed self-deactivation at physiological temperatures, positioning it as a prime candidate for pharmacological chaperone therapy in Gaucher disease. Additionally, our results illustrate that chemical tailoring enables the engineering of photocommutators with the ability to toggle inhibition between α- and β-glucosidase enzymes in a reversible manner, thus expanding the versatility and potential therapeutic applications of this approach.

1. Introduction

Phototransformable molecules based on photochromism chemistry provide opportunity to manipulate biological activity with remarkable accuracy in both timing and location. [1–3] Azobenzene and its derivatives stand out within this category. These compounds consist of two phenyl rings connected by a N=N double bond.[4] Notably, the two isomeric forms, *E* and *Z*, can be toggled using specific light wavelengths. Typically, in the case of 2,2′- or 4,4′-disubstituted azobenzene derivatives ultraviolet (UV) light (at ~ 365 nm) facilitates the *trans*-to-*cis* conversion, while visible light (at ~ 465 nm) instigates the *cis*-to-*trans* isomerization process. The later process is thermodynamically favored and also occurs in the dark at a temperature-dependent rate. Nevertheless, the nature of the substituents and the substitution pattern at the azobenzene system greatly influence the thermodynamic stability, photochemical properties and absorption spectra, which can be leveraged to customize from UV- to visible-light-sensitive molecules.[5] This strategy has been embraced for the creation of photoswitchable lipids, [6] ligands, [7–10] nucleic acids,[11] ion channels,[12,13] and a diverse array of other biomolecules.[14,15] Despite this, the assortment of bioactive molecules endowed with photo-controlled attributes remains relatively modest. [16] A main obstacle revolves around achieving substantial differentials in activity between the photoisomeric forms. In the best possible scenario, one isomer does not change the activity of the protein of interest, while the alternate isomer leads to a comprehensive suppression of protein function. This would permit the protein to be toggled entirely between an active and inactive state.

* Corresponding author.
E-mail addresses: joanne.xie@ens-paris-saclay.fr (J. Xie), jogarcia@iiq.csic.es (J.M. García Fernández), mellet@us.es (C. Ortiz Mellet).

https://doi.org/10.1016/j.bioorg.2024.107555
Received 30 March 2024; Received in revised form 3 June 2024; Accepted 10 June 2024
Available online 12 June 2024

The above ideal situation of complete switching is seldom realized in practice. The regulation of enzyme activity illustrates these notions: optical control over enzyme function can be achieved by installation of molecular photoswitches into the scaffold of enzyme inhibitors. Yet, the switching factor (SF), i.e., the ratio between the inhibition constants of the *cis* and *trans* isomer, is often suboptimal, typically less than one order of magnitude. [17] Most of successful examples showcasing effective light-controlled enzyme activity regulation pertain to the realm of proteases, the enzymes that have been targeted the most by photoswitchable inhibitors.[18–20] Somehow unexpectedly, the literature reflects a patent scarcity of accounts concerning photoactive glycosyl hydrolase (glycosidase) actuators, and the available reports suggest relatively modest SF values. Thus, König and coll. reported the synthesis of a remarkably potent β-galactosidase-inhibitory photochromic compound, **1**, an azobenzene β-D-thiogalactopyranoside derivative (Fig. 1). This compound showed 4.8-fold difference upon switching from the *E*-isomer (inhibition constant, $K_i = 60$ nM) to the *Z*-isomer ($K_i = 290$ nM). [21].

Matassini, Cacciarini and coll. [22] prepared mono and divalent conjugates of a specific trihydroxypiperidine and azobenzene, namely compounds **2** and **3** (Fig. 1). These compounds were designed as inhibitors targeting human lysosomal β-glucocerebrosidase (GCase). The dysfunction of this enzyme, often linked to mutations causing misfolding and premature degradation within the endoplasmic reticulum (ER), underlies the genesis of Gaucher disease (GD), the most prevalent lysosomal storage disorder (LSD). The ratios of inhibitory potency (IC_{50} values) between the *E* and *Z* isomers of compounds **2** and **3** remained relatively modest, at 4.7 and approximately 1, respectively. The closely analogous compounds **4** and **5** (Fig. 1), possessing elongated aliphatic spacers, showed SF values in the same range, 1.7 and 2.3, respectively. [23].

The preceding discussion highlights the challenges encountered in the development of glycosidase inhibitors suitable for photopharmacological applications. A primary obstacle lies in the fact that glycosidase selectivity is primarily governed by interactions within the glycone binding site, where the sugar moiety of the natural substrate binds. Conversely, the regions accommodating aglycone and non-glycone substituents exhibit relatively lower demands for structural compatibility, which poses difficulties in inducing high SF values by *E*/*Z* isomerization of azobenzene modules appended on sugar-like

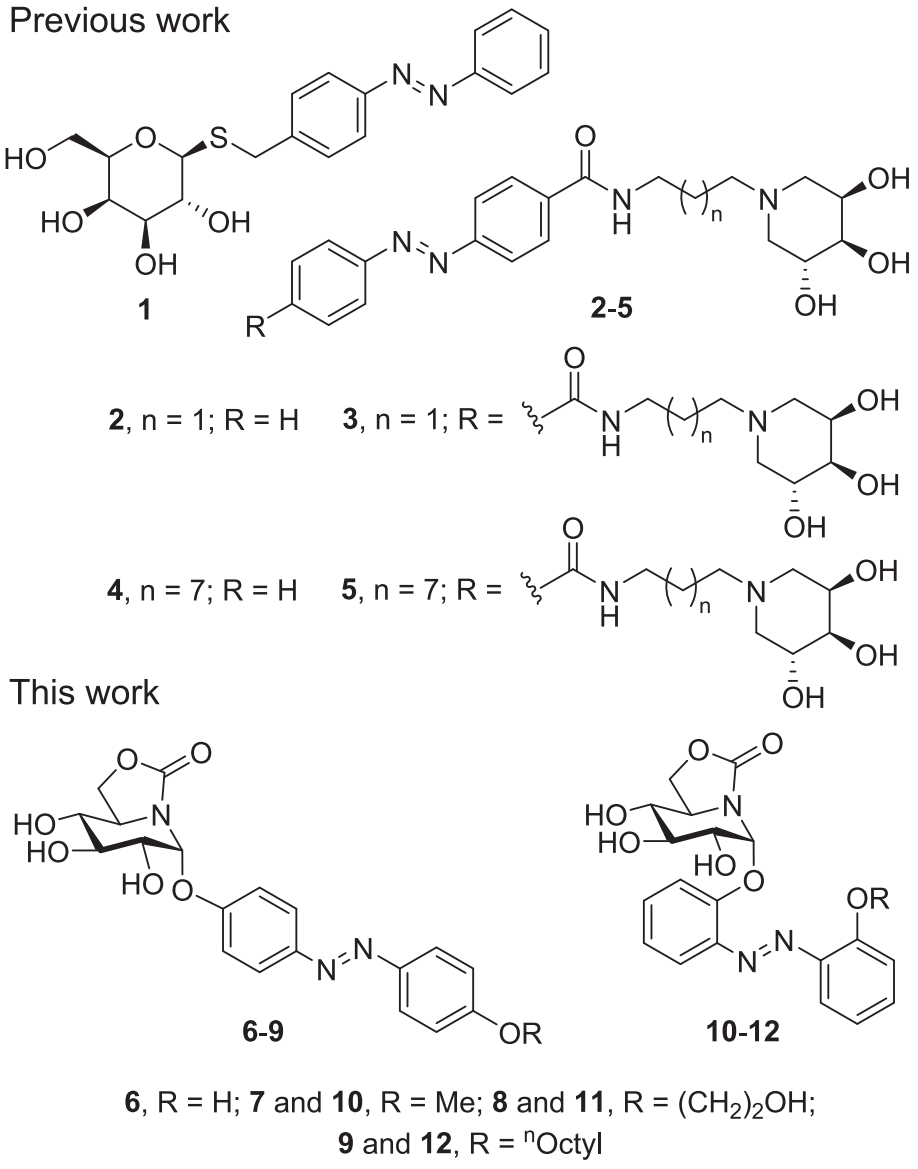

Fig. 1. Structures of the photoswitchable glycosidase inhibitors previously reported, namely the azobenzene-thioglycoside **1** and the trihydroxypiperidine-azobenzene conjugates **2**–**5**, and of the 5*N*,6*O*-oxomethylidenenojirimycin (ONJ)-azobenzene conjugates **6**–**12** reported in this work.

frameworks. A second limitation emerges from observations that, in the reported instances, the thermodynamically more stable *E*-isomer consistently displays greater activity compared to the *Z*-isomer. Consequently, inducing dissociation of the enzyme-inhibitor complex necessitates light irradiation, a constraint that is impractical within real clinical scenarios. However, this predicament may not apply in the case of pseudoamide-type nitrogen-in-the-ring glycomimetic derivatives of the sp^2-iminosugar category. [24–30] The effectiveness of sp^2-iminosugars as glycosidase inhibitors is closely intertwined with the presence or absence of a glycone-like moiety and the identity plus orientation of exocyclic substituents, including aglycon modules in pseudoglycoside derivatives. [31,32] We propose that integrating an azobenzene photoswitch at this specific region could yield substantial variations in inhibition potency upon photoisomerization. Furthermore, the synthesis of sp^2-iminosugars can be readily adapted to strategies promoting molecular diversity, thus expediting the identification and optimization of candidates exhibiting desired pharmacological traits. [33,34] Of particular interest is attaining a high ratio of inhibitory activity against a medically relevant enzyme, favoring the *Z* form over the *E* form, while also ensuring a thermal return half-life compatible with the expression of the desired beneficial effect and mitigating the undesired accumulation of the inhibitor. [35].

To explore this hypothesis, a series of 5*N*,6*O*-oxomethylidenenojirimycin (ONJ)-azobenzene conjugates has been synthesized (compounds **6**–**12**; Fig. 1), and their responses to photochemical stimuli were monitored. Glycosides of the sp^2-iminosugar ONJ mirror the configurational pattern of the D-glucoside counterparts, the putative substrates of glucosidases. Exploration of their glycosidase inhibition properties revealed compound **9** as a promising candidate for modulating the activity of human GCase by the action of light and temperature in the context of Gaucher disease.

2. Results and discussion

2.1. Synthesis of o-glycosylated p/o-azobenzene-ONJ derivatives

The distinctive stereoelectronic attributes of sp^2-iminosugars, marked by a heightened anomeric effect, empower their participation as glycosyl donors in glycosylation reactions, facilitating the formation of α-glycosides with impeccable stereoselectivity. Pseudo-*O*-, *S*-, *N*-, and *C*-glycosides have been thus accessed.[25,28,36,37] In the present work, the synthesis of the glycosyl acceptors required for the preparation of the azobenzene-containing sp^2-iminosugar pseudo-*O*-glycosides **6**–**12** implied the monoalkylation of the commercial reagents 4,4′- (**13**) and

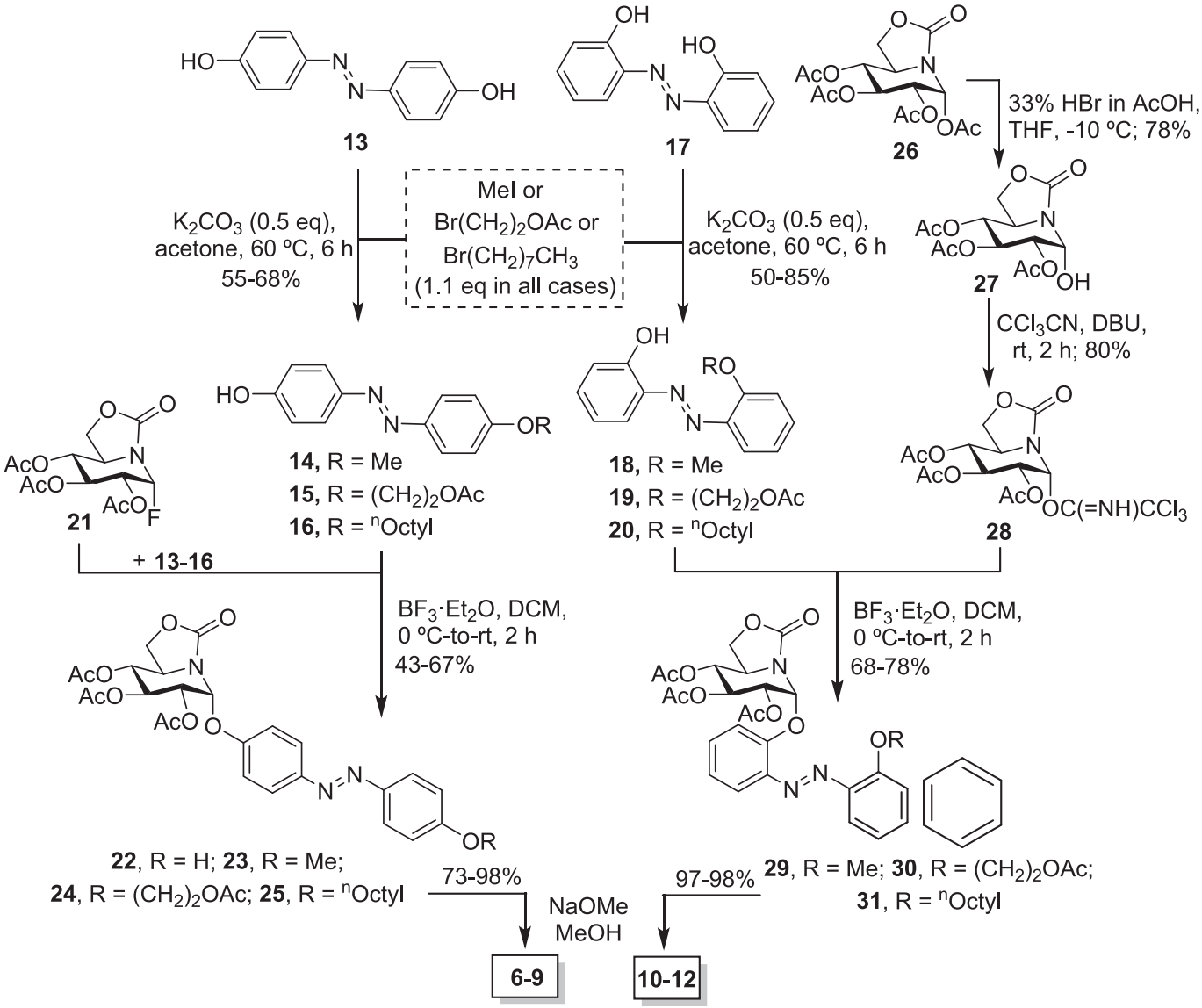

Scheme 1. Synthesis of the *p*- and *o*-azobenzene ONJ pseudo-*O*-glycosides **6**–**12**.

2,2′-dihydroxyazobenzene (**17**). Statistical reactions were carried out using a default base (potassium carbonate, 0.5 eq/mol azobenzene) and a slight excess of alkylating reagent (methyl iodide, 2-bromoethyl acetate or octyl bromide, 1.1 eq/mol azobenzene) in acetone at 60 °C. The corresponding monophenols **14**, [38] **15**, **16** [39] and **18**, **19**, **20** (see the SI for synthetic details) were isolated in 55–68 % and 50–85 % yield, respectively (Scheme 1).

The combination of a pseudoglycosyl fluoride, such as the ONJ derivative **21** [40] (D-*gluco*-configured) as glycosyl donor and boron trifluoride etherate ($BF_3{\cdot}Et_2O$) as glycosylation promotor has proven particularly efficient to access the corresponding pseudo-*O*-gycosides in previous reports. [41–43] Hence, we initially adopted this strategy for the preparation of azobenzene-containing sp^2-iminosugar glycosides. Glycosylation reactions between **21** and the *p*-azobenzene acceptors **14**–**16** under such conditions led to the corresponding pseudoglycosides **23**–**25**. A statistic monoglycosylation of **13** was also performed to get **22**, keeping a free phenolic hydroxyl. Deacetylation of **22**–**25** using catalytic 1 M MeONa in MeOH afforded the target fully unprotected compounds **6**–**9** with yields ranging from 73 to 98 % (Scheme 1). In the ^{1}H NMR spectra, four signals are observed in the region 7.91–7.02 ppm, corresponding to the aromatic protons of the *para*-disubstituted azobenzene system. It is also worth noting the doublet located at 5.75 ppm, ascribable to the pseudoanomeric proton (H-1); the coupling constant value (3.9 Hz) supports the α-anomeric configuration. In the ^{13}C NMR spectra, the nine signals in the region 161.6–115.4 ppm can be assigned to the eight magnetically inequivalent aromatic carbons of the *para*-disubstituted azobenzene module and the carbonyl carbon characteristic of the carbamate group (159.1 ppm; see Supporting Information Fig. S1 to S18 for copies of the NMR and MS spectra).

Attempts to extend the above strategy to the preparation of *o*-azobenzene derivatives were unsuccessful. Only hydrolysis of the pseudoglycosyl fluoride **21** was observed after longer reaction times. As an alternative, the use of the corresponding ONJ pseudoglycosyl trichloroacetimidate derivative **28** [44] was envisioned (Scheme 1). The preparation involved the selective deprotection of the pseudoanomeric position in the ONJ per-*O*-acetate **26** [45] to give compound **27**. The use of hydrazinium acetate in DMF [46] as well as $FeCl_3$ in MeCN [47] afforded only modest (<50 %) yields of the target hemiacetal. Gratifyingly, using HBr (33 %) in glacial AcOH and THF as the solvent led to the desired compound in 78 % yield. Subsequent treatment of **27** with trichloroacetonitrile in DCM, using DBU as a base catalyst, provided **28**, which upon reaction with acceptors **18**—**20** in the presence of $BF_3{\cdot}Et_2O$ (0.3 eq) afforded the α-configured *o*-azobenzene ONJ pseudoglycosides **29**–**31** in 68–78 % yield. Subsequent Zemplén deacetylation delivered the target unprotected glycoside mimetics **10**–**12** in virtually quantitative yield (Scheme 1).

2.2. Photocharacterization studies of p/o-azobenzene ONJ pseudoglycosides

For the photocharacterization of the *p*/*o*-azobenzene ONJ pseudoglycosides **6**–**12**, stock solutions of each derivative were prepared in DMSO and kept in the dark at 25 °C overnight to ensure full *Z*-to-*E* conversion. The stock solution, containing almost exclusively the *E*-isomer, was used directly to investigate the properties of this isomer. For *Z*-isomer measurements, the sample was irradiated for 1 min at 365 nm, near the absorption maximum for the *E*-isomer, to reach the photostationary state (PSS). The exception is compound **6**, bearing a free phenolic hydroxyl on the *p*-azobenzene system. In this case, we observed low $E \rightarrow Z$ photoconversion yields, with the compound returning to the thermodynamically more stable *E* configuration after only 4 min at 37 °C in DMSO (Supporting information, Fig. S62). This phenomenon occurred due to the tautomeric equilibration between the azo-phenol and quinone-hydrazone forms.[48] The later form is favored by the presence of the electron-withdrawing ONJ pseudoglycosyl substituent, leading to fast rotation around the N — N bond to the more stable *E* isomer. Similar fast thermal $Z \rightarrow E$ isomerization processes were previously observed in monoglycosylated derivatives of compounds **13** and **17**.[49,50].

Compounds **7**–**9** showed quite similar spectroscopic and kinetic properties. After irradiation of a solution of the *E* isomer in DMSO at 365 nm ($P = 7.5$ mW·cm^{-2}), the characteristic band at 360–361 nm vanishes and a maximum at 447–448 nm shows up, with isosbestic points located at 315–319 nm and 419–420 nm (Table 1; see also the Supporting Information, Fig. S63-S65). Photoisomerization of the *E* to the *Z* isomer was essentially total (>97 %), as gauged by ^{1}H NMR spectroscopy. As an illustrative example, the corresponding spectra for compound **7** before and after irradiating the sample at 365 nm are depicted in Fig. 2 (see also Supporting information, Fig. S69). Upon reaching the PSS_{365}, the signals located at 7.82, 7.22, and 7.40 ppm, corresponding to the aromatic protons of the azobenzene group in its *E* configuration, disappear. Instead, new signals at 6.90 and 6.80 ppm, corresponding to the *Z*-isomer, become apparent. The chemical shifts of the sp^2-iminosugar unit protons are also shifted, indicative of a change in their magnetic environment. The integrals of the signals from both isomers confirm quantitative photoconversion.

Irradiation of the DMSO solutions of **7**–**9** containing the *Z*-isomer at 514 nm ($P = 5.4$ mW·cm^2) for 10 min led to a near-total (>85 %) recovery of the *E* isomer. In the dark, at 37 °C, the solutions of the metastable *Z*-isomer derivatives showed half-lives ($\tau_{1/2}$) of 246 to 269 min (Table 1; see also the Supporting Information, Fig. S63-S65). This $\tau_{1/2}$ values are judged sufficient to warrant a significant proportion of the *Z* isomer in subsequent glycosidase inhibition assays against glycosidases, where the estimated incubation time with the enzyme is 10 min.

In the case of the ortho derivatives **10**–**12**, a bathochromic shift of the absorption maximum as compared with the *p*-azobenzene positional isomers was observed, with absorption maxima between 367 and 371 nm. In addition, the molar absorption coefficients are reduced by approximately half (8686–15224 for **10**–**12** vs 22919–28930 L·mol^{-1}·cm^{-1} for **7**–**9**). After irradiation of DMSO solutions at 365 nm, the band corresponding to this maxima fades, with the simultaneous appearance of a single isosbestic point at 277–278 nm. These data align with an almost complete *E*-to-*Z* conversion, as confirmed by NMR analysis. In these systems, the highest photochemical recovery of *E* isomer is obtained by irradiating the sample at 438 nm, with *Z*-to-*E* photoconversion yields of 62–65 %. The high thermal stability of the *Z*-configured *ortho*-substituted derivatives is also noteworthy. Thus, kinetic studies showed $\tau_{1/2}$ values > 24 h, about ten-fold higher than those determined for the corresponding *para* compounds. This difference is likely due to the steric hindrance induced by *ortho*-substitution (Table 1; see also the Supporting Information, Fig. S66-S68).

2.3. Evaluation of the activity of p/o-azobenzene ONJ pseudoglycosides as inhibitors of glycosidases

Before conducting the inhibition assays, control experiments were undertaken to evaluate the *Z*-to-*E* azobenzene conversion under the specific conditions employed for determining the inhibitory activity of glycosidases. Compound **7**, baker's yeast α-glucosidase, and 4-methylumbelliferyl α-D-glucopyranoside were employed as the light-sensitive inhibitor, control enzyme, and reference substrate, respectively, for this assessment. Previous results informed that this enzyme is particularly susceptible to competitive inhibition by α-configured ONJ glycoside mimetics.[51–53] A stock solution of the *E* isomer of **7** (2 mM) in DMSO was prepared and used directly in the assay by adding buffer, substrate and milliQ® H_2O to reach a final proportion of 10 % DMSO in H_2O. Incubation times and protocols matched those used in a typical inhibition constant (K_i) determination assay (see Supporting Information). For the *Z* isomers, the stock solution in DMSO was first irradiated at 365 nm ($P = 5.4$ mW·cm^{-2}) for 10–15 min in order to promote *E*-to-*Z* photoconversion, which was monitored by UV–vis absorption, and the sample was processed similarly. At the end of the experiment, the

Table 1
Photophysical and photochemical parameters for the *E* ↔ *Z* photoisomerization of the *p*/*o*-azobenzene ONJ pseudoglycosides **7**–**9** and **10**–**12** in DMSO.

Compound	λ_{max}(nm)		Isosbestic points (nm)	$\varepsilon_{\lambda max}$ ($L \cdot mol^{-1}\ cm^{-1}$)	$\tau_{1/2}$ 37 °C	Photoconversion yield (%)[a]	
	E	*Z*				*E*→*Z*	*Z*→*E*
7	360	448	315, 419	28,917	269 min	>97	90
8	361	447	319, 429	28,617	269 min	>97	99
9	361	447	319, 420	22,919	246 min	>97	85
10	367	–	278	11,370	>24 h	>97	62
11	368	–	277	15,224	>24 h	>97	64
12	371	–	278	8686	>24 h	>97	65

[a] Photostationary distribution (PSD) assessed by ^{1}H NMR.

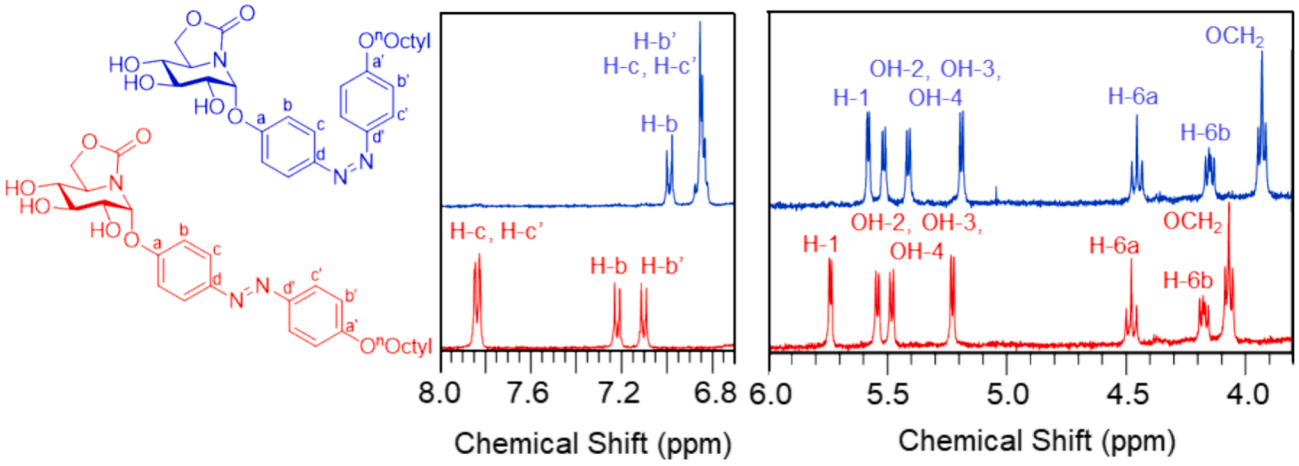

Fig. 2. Aromatic (left) and ONJ (right) proton regions in the ^{1}H NMR spectra of **9** in $(CD_3)_2SO$ before (*E*-isomer, red line) and after irradiation at 365 nm (*Z*-isomer, blue line). The full spectra for both isomers are provided in the Supporting Information, Figure S69. (For interpretation of the references to colour in this figure legend, the reader is referred to the web version of this article.)

proportion of the *E* and *Z* isomer was determined by UHPLC-MS (Table 2). The data confirmed that photoconversion or thermal conversion was not affected by the presence of the enzyme or the substrate, thereby validating the method and the reliability of the inhibition constants thus obtained.

The inhibitory potential of the whole series of photoswitchable *p*- and *o*-azobenzene glycoside mimetics **6**–**12** was subsequently checked against the control baker's yeast α-glucosidase. As anticipated, all compounds demonstrated robust competitive inhibition of the enzyme, with inhibition constant (K_i) values ranging from 6.1 to 91.5 μM for *p*-azobenzene derivatives (**6**–**9**) and from 0.15 to 0.85 μM for *o*-azobenzene derivatives (**10**–**12**). Consistent with existing literature, [18–20] the extended *E*-isomer generally exhibited greater efficacy compared to the twisted *Z*-isomer. However, a notable dependence of the SF value on the aglycone structure, particularly the distal azobenzene substituent, was observed. The 2-hydroxyethyloxy derivatives **8** and **11** were notably sensitive to light-induced photoisomerization, evidenced by K_i (*Z*)/ K_i (*E*) ratios of 7.7 and 5.7, respectively. Notably, the 4′-octyloxyazobenzene ONJ glycoside **9** deviated from the expected trend, as the inhibitory potency of its *Z*-isomer (K_i 11.4 μM) surpassed that of the *E*-isomer (K_i 25.5 μM), yielding an SF value of 0.4 (Table 3).

The data presented above reaffirmed the notion that sp^2-iminosugar azobenzene glycosides serve as advantageous frameworks for designing light-responsive glycosidase inhibitors. Of particular interest is the potential to identify compounds with significant selectivity favoring the less stable Z-isomer. Such molecules could be activated upon irradiation at the appropriate wavelength and would then undergo controlled self-deactivation within a time frame determined by their respective half-lives. To further investigate this concept, we conducted a subsequent analysis to evaluate the inhibitory capabilities of compounds **6**–**12** against a panel of commercial glycosidases. This panel included α-glucosidase from *Oryza sativa* (rice), β-glucosidases from bovine liver, almonds, and *Thermotoga maritima*, α- and β-galactosidases from green coffee beans and *Escherichia coli*, and α- and β-mannosidases from Jack beans and *Helix pomatia*, respectively. The selection of α- and β-glucosidase representatives was based on their classification in the glycosyl hydrolase families GH31 and GH1 in the Carbohydrate Active Enzyme (CAZy) database. [54] These families also include human lysosomal

Table 2
Validation of the protocol for glycosidase inhibition evaluation of the photoswitchable sp^2-iminosugar **7** against baker's yeast α-glucosidase.

Control test	**7**[a] (μL)	Buffer[b] (μL)	Substrate[c] μL)	MilliQ® H_2O (μL)	Enzyme[d] (μL)	Not irradiated[e] (%)[g]		Irradiated[f] (%)[g]	
						E	*Z*	*E*	*Z*
1	10	15	–-	75	–-	>98	n.d.[h]	5	95
2	10	15	25	50	–-	>97	n.d.	6	94
3	10	15	25	40	10	>98	n.d.	5	96
4	10	40	–-	40	10	>98	n.d.	7	93

[a] 2 mM in DMSO. [b]PBS 1 M, pH 6.8.[c]4-Methylumbelliferyl α-D-glucopyranoside (1 mM in PBS buffer). [d]0.98 $U \cdot mL^{-1}$ (~0.1 $mg \cdot mL^{-1}$). [e]Sample prepared from a stock solution of the *E*-isomer of **7** in DMSO after heating at 60 °C overnight. [f]Sample prepared by irradiating the stock solution of the *E*-isomer of **7** at 365 nm (P = 7.5 $mW \cdot cm^{-2}$) for 15 min in order to promote *E*-to-*Z* photoconversion. [g]Relative isomeric ratio determined by UHPLC-MS. [h]Not detected.

Table 3
Inhibition constants (K_i, μM) of the azobenzene ONJ pseudoglycosides **6**–**12** (the nature of the non-pseudoglycosidic substituent is indicated).[a-c]

Comp.	Isomer	Baker's yeast α-glucosidase		*Oryza sativa* α-glucosidase		Bovine liver β-glucosidase	
		K_i (μM)	SF[d]	K_i (μM)	SF	K_i (μM)	SF
6 (*p*-OH)	*E*	6.1 ± 0.5	–-	276 ± 22	–-	41.1 ± 3.4	–-
7 (*p*-OMe)	*E*	21.7 ± 2.0	1.6	n.i.[e]	–-	n.i.	–-
	Z	35.5 ± 3.2		n.i.		n.i.	
8 (*p*-O $(CH_2)_2OH$)	*E*	11.9 ± 1.0	7.7	n.i.	–-	4.5 ± 0.4[f]	1.02
	Z	91.5 ± 8.8		n.i.		4.4 ± 0.4 [g]	
9 (*p*-O $(CH_2)_7CH_3$)	*E*	25.5 ± 2.1	0.4	n.i.	–-	n.i.	<0.06
	Z	11.4 ± 1.1		n.i.		60.7 ± 5.9	
10 (*o*- OMe)	*E*	0.56 ± 0.05	1.1	375 ± 28	0.32	142 ± 14	0.31
	Z	0.64 ± 0.06		120 ± 11		44.2 ± 3.9	
11 (*o*-O $(CH_2)_2OH$)	*E*	0.15 ± 0.01	5.7	176 ± 14	0.07	56.5 ± 5.5	1.3
	Z	0.85 ± 0.07		13.0 ± 2		76.0 ± 7.0	
12 (*o*-O $(CH_2)_7CH_3$)	*E*	0.74 ± 0.06	1.2	n.i.	–-	34.4 ± 2.7	0.77
	Z	0.87 ± 0.08		n.i.		26.4 ± 3.1	

[a]Values represent the mean ± SD (n = 3). [b]No inhibitory activity (K_i > 1000 μM) was observed against α-galactosidase (green coffee bean), β-galactosidase (*E. Coli*), α-mannosidase (Jack bean) and β-mannosidase (*Helix pomatia*). [c]The *p*-azobenzene ONJ conjugates **6**–**9** showed no inhibitory activity against almonds and *Thermotoga maritima* β-glucosidases, whereas the *o*-azobenzene derivatives **10**–**12** behaved as poor inhibitors for these enzymes, with K_i values > 300 μM. [d]Switching factor, defined as the ratio between the K_i values for the *E* and the *Z*-isomer. [e]n.i., no inhibition observed at 1 mM concentration of the inhibitor (K_i > 1000 μM). [f]Inhibition constant for the enzyme-inhibitor (E-I) binding of uncompetitive inhibition mode. [g]Inhibition constant for the E-I binding of non-competitive inhibition mode.

α-glucosidase and GCase, whose dysfunction is associated with the lysosomal storage disorders Pompe and Gaucher disease, [55] respectively, implying similarity in active site architecture.

The results, summarized in Table 3, confirmed a clear preference for glucosidase enzymes over galactosidases and mannosidases, highlighting ONJ conjugates as effective mimics of glucopyranosides. It is noteworthy that all compounds in the series, excepting compound **7**, exhibited inhibitory activity against GH1 β-glucosidases, particularly the mammalian isoenzyme, despite their fixed α-anomeric configuration. Although seemingly counterintuitive, previous evidence has demonstrated that α-configured glycomimetics can adopt a skew-boat conformation within the active site of β-glucosidase, allowing the pseudoanomeric substituent to assume a pseudoequatorial disposition. [56,57] The *p*-2-hydroxyethyloxy derivative **8**, regardless of its *E* or *Z* configuration, exhibited potent inhibition. Intriguingly, the inhibition mechanism shifted from uncompetitive for the *E*-isomer to non-competitive for the *Z*-isomer (Supporting Information, Fig. S32 and S33), suggesting that the former binds to the enzyme-substrate complex, while the latter interacts with regions of the enzyme distinct from the active site. In all other cases, the inhibition mode observed was competitive (Supporting Information, Fig. S19–S31 and S34–S59).

Of particular note, the 4′-octyloxyazobenzene glycoside **9** selectively inhibited the β-glucosidase enzyme in its *Z*-form (K_i 60.7 ± 5.9 μM), while showing no activity in its *E*-form. To the best of our knowledge, this marks the first instance of a photoswitchable glycosidase inhibitor with a total on–off switching behavior. We therefore selected this compound to gauge its potential as human GCase pharmacological chaperone (PC). PCs, are small molecules having the capability to promote the correct folding of disease-associated mutant enzyme variants at the endoplasmic reticulum, prevent premature degradation and restore trafficking to the lysosome. [58,59] In a significant number of GD patients, the mutant enzyme retains catalytic competence, and its activity can be reinstated if the PC, typically a competitive inhibitor, subsequently dissociates from the enzyme-inhibitor complex at an appropriate rate. We found that **9**-*Z* (K_i 1.07 ± 0.11 nM; see the Supporting Information, Fig. S61) exhibited over a $2.5{\cdot}10^3$-fold greater inhibitory potency against human GCase than **9**-*E* (K_i 2.80 ± 0.27 μM; see the Supporting Information, Fig. S60). Given the gradual *Z*-to-*E* azobenzene isomerization at physiological temperature ($\tau_{1/2}$ 246 min at 37 °C; Table 1), the compound functions as a self-deactivating GCase inhibitor. Considering the critical importance of maximizing the chaperone versus inhibitor characteristics of PCs for clinical use, [60] these findings underscore the promising potential of photoactivable sp^2-iminosugars as agents capable of precisely regulating glycosidase targets through control of light and temperature conditions.

Among the compounds tested, only the *o*-azobenzene glycosides **10** and **11** inhibited the *Oryza sativa* GH31 α-glucosidase. Significantly, the *Z*-isomer demonstrated superior inhibitory potency compared to the *E*-isomer, with compound **11** standing out with a switching factor of 0.07, indicating that **11**-*Z* (K_i 13 μM) is over 13.5-fold more effective than **11**-*E* (K_i 176 μM) towards this enzyme. Opposite to this trend, **11**-*E* was a more potent inhibitor of the bovine liver β-glucosidase (K_i 56.5 μM) compared to **11**-*Z* (K_i 76.0 μM). In practical terms, these results suggest that photoisomerization does not function merely as a simple on–off switch in this context, but rather as a commutator between two distinct active states: from selective inhibition of β-glucosidase to selective inhibition of α-glucosidase. This presents a unique model system for exploring light-induced control of enzyme activity.

3. Conclusions

We have refined the synthesis of photoswitchable *p*- and *o*-azobenzene α-glycoside mimetics based on the sp^2-iminosugar ONJ. Employing the ONJ pseudoglycosyl fluoride as the glycosyl donor and boron trifluoride etherate as the promoter proved to be highly efficient for generating the desired *p*-azobenzene α-pseudoglycosides. However, to access the *o*-azobenzene pseudoglycosides, we required the use of the more reactive ONJ anomeric trichloroacetimidate. The *E* and *Z* isomers at the azo group in the final α-pseudoglycosides showed photo and thermal stability compatible with the classical protocol for determination of glycosidase inhibition properties. This was confirmed through testing against the α-glucosidase from baker's yeast as a control enzyme. Further screening the compounds against a panel of glycosidases with varied configurational specificities highlighted their distinct glucopyranoside mimicking nature. Notably, no off-target inhibition of galactosidases or mannosidases was observed. Most significantly, we achieved unprecedentedly high switching factors favoring either the *E*- or *Z*-isomer, depending on the aglycone structure. The data also revealed a correlation between the isomeric state of the azobenzene module and the selectivity towards α- and β-glycosidase isoenzymes that are structurally akin to corresponding human lysosomal glycosidases. Most significantly, compound **9** was singled-out as a reversible inhibitor of human GCase with a 1/2500 *E*-to-*Z* switching factor.

The significance of this research concerning glycosidase activity photocontrol for biomedical applications unfolds on dual fronts. Firstly, our findings demonstrate the remarkable capability of sp^2-iminosugar azobenzene conjugates to be tailored, emphasizing a distinct preference for inhibiting the target enzyme via the *Z*-isomer, thereby facilitating ex-vivo drug activation and programmed self-deactivation under thermal conditions. Secondly, our results elucidate how chemical tailoring enables the engineering of photocommutators, affording the ability to

switch from inhibiting one glycosidase to another in a reversible manner, thus expanding the versatility and potential therapeutic applications of this approach.

4. Experimental section

Experimental details are provided as Supplementary data.

CRediT authorship contribution statement

Gonzalo Rivero-Barbarroja: Writing – review & editing, Validation, Methodology, Investigation. **M. Carmen Padilla-Pérez:** Writing – review & editing, Investigation. **Stéphane Maisonneuve:** Writing – review & editing, Validation, Supervision, Methodology, Formal analysis, Data curation, Conceptualization. **M. Isabel García-Moreno:** Writing – review & editing, Validation, Supervision, Methodology, Formal analysis, Data curation. **Ben Tiet:** Methodology, Investigation. **David J. Vocadlo:** Writing – review & editing, Validation, Supervision, Resources, Funding acquisition, Conceptualization. **Juan Xie:** Writing – review & editing, Supervision, Resources, Funding acquisition, Conceptualization. **José M. García Fernández:** Writing – original draft, Supervision, Funding acquisition, Conceptualization. **Carmen Ortiz Mellet:** Writing – original draft, Validation, Supervision, Resources, Funding acquisition, Conceptualization.

Declaration of competing interest

The authors declare that they have no known competing financial interests or personal relationships that could have appeared to influence the work reported in this paper.

Acknowledgements

We acknowledge the Ministerio de Ciencia, Innovación y Universidades and the Agencia Estatal de Investigación, AEI/10.13039/501100011033 and "ERDF A way of making Europe'' (PID2021-124247OB-C21 and PID2022-141034OB-C21), the COST action GLYCONanoPROBES (CM18132), and the Booster program of ENS Paris-Saclay for financial support. DJV thanks the Natural Sciences and Engineering Research Council of Canada (RGPIN-2020-06466) for financial support and the Canada Research Chairs for a Tier I Canada Research Chair in Chemical Biology. We also acknowledge the CITIUS (Univ. Seville), for technical support. G.R.-B and M.C.P.-P. were FPU fellows (Grant numbers FPU18/02922 and FPU19/04361, respectively).

Appendix A. Supplementary data

Synthetic methods, UV-Vis spectroscopy methods, NMR and MS spectra, glycosidase inhibition methods, including the corresponding Lineweaver-Burk and Dixon plots, and additional UV-Vis spectra (PDF). Supplementary data to this article can be found online at https://doi.org/10.1016/j.bioorg.2024.107555.

References

[1] J. Broichhagen, J. Allen Frank, D. Trauner, A Roadmap to Success in Photopharmacology, Acc. Chem. Res. 48 (7) (2015) 1947–1960.
[2] K. Hull, J. Morstein, D. Trauner, *In Vivo* Photopharmacology, Chem. Rev. 118 (2018) 10710–10747.
[3] M.J. Fuchter, On the Promise of Photopharmacology Using Photoswitches: A Medicinal Chemist's Perspective, J. Med. Chem. 63 (2020) 11436–11447.
[4] K.G. Yager, C.J. Barrett, Novel photo-switching using azobenzene functional materials, J Photochem. Photobiol. a. 18 (2006) 250–261.
[5] M. Gao, D. Kwaria, Y. Norikane, Visible-light-switchable azobenzenes: Molecular design, supramolecular systems, and applications, Nat. Sci. (2023) e220020.
[6] G.J. Mohr, A tricyanovinyl azobenzene dye used for the optical detection of amines via a chemical reaction in polymer layers, Dyes Pigm. 6 (2004) 7–81.
[7] W.R. Browne, B.L. Feringa, Making molecular machines work. *Nat*, Nano 1 (2006) 25–35.
[8] X.G. Liang, H. Nishioka, N. Takenaka, H. Asanuma, A DNA nanomachine powered by light irradiation, ChemBioChem. 9 (2008) 702–705.
[9] M. Yamada, M. Kondo, J. Mamiya, Y. Yu, M. Kinoshita, C.J. Barrett, T. Ikeda, Photomobile polymer materials: Towards light-driven plastic motors, Angew. Chem. Int. Ed. 47 (2008) 4986–4988.
[10] C. Dugave, Cis-trans Isomerization in Biochemistry, Wiley-VCH, New York, 2006.
[11] M. Bose, D. Groff, J. Xie, E. Brustad, P.G. Schultz, The incorporation of a photoisomerizable amino acid into proteins in E. coli, J. Am. Chem. Soc. 128 (2006) 388–389.
[12] G.A. Woolley, Photocontrolling peptide alpha helices, Acc. Chem. Res. 38 (2005) 486–493.
[13] D.L. Robertson, G.F. Joyce, Selection in vitro of an RNA enzyme that specifically cleaves single-stranded-DNA, Nature 344 (1990) 467–468.
[14] N.L. Mutter, J. Volarić, W. Szymanski, B.L. Feringa, G. Maglia, Reversible photocontrolled nanopore assembly, J. Am. Chem. Soc. 141 (2019) 14356–14363.
[15] R. Ando, H. Mizuno, A. Miyawaki, A., Regulated fast nucleocytoplasmic shuttling observed by reversible protein highlighting, Science 306 (2004) 1370–1373.
[16] M.M. Lerch, M.J. Hansen, G.M. van Dam, W. Szymanski, Emerging targets in photopharmacology, Angew. Chem. Int. Ed. Engl. 55 (2016) 10978–10999.
[17] M. Teders, A.A. Pogodaev, G. Bojanov, W.T.S. Huck, Reversible photoswitchable inhibitors generate ultrasensitivity in out-of-equilibrium enzymatic reactions, J. Am. Chem. Soc. 143 (2021) 5709–5716.
[18] M. Zhu, H. Zhou, Azobenzene-based small molecular photoswitches for protein modulation, Org. Biomol. Chem. 16 (2018) 8434–8445.
[19] C. Claaßen, T. Gerlach, D. Rother, Stimulus-Responsive Regulation of Enzyme Activity for One-Step and Multi-Step Syntheses, Adv. Synth. Catal. 361 (2019) 2387–2401.
[20] L. Josa-Cullere, A. Llebaria, Visible-light-controlled histone deacetylase inhibitors for targeted cancer therapy, J. Med. Chem. 66 (2023) 1909–1927.
[21] K. Rustler, M.J. Mickert, J. Nazet, R. Merkl, H.H. Gorris, B. König, Development of photoswitchable inhibitors for β-galactosidase, Org. Biomol. Chem. 16 (2018) 7430–7437.
[22] M.G. Davighi, F. Clemente, C. Matassini, F. Cardona, M.B. Nielsen, A. Goti, A. Morrone, P. Paoli, M. Cacciarini, Photoswitchable inhibitors of human β-glucocerebrosidase, Org. Biomol. Chem. 20 (2022) 1637–1641.
[23] F. Clemente, M.G. Davighi, C. Matassini, F. Cardona, A. Goti, A. Morrone, P. Paoli, T. Tejero, P. Merino, M. Cacciarini, Light-triggered control of glucocerebrosidase inhibitors: Towards photoswitchable pharmacological chaperones, Chem. Eur. J. 29 (2023) e202203841.
[24] J.L. Jiménez Blanco, V.M. Díaz Pérez, C. Ortiz Mellet, J. Fuentes, J.M. García Fernández, J.C. Díaz Arribas, F.J. Cañada, *N*-Thiocarbonyl azasugars: A new family of carbohydrate mimics with controlled anomeric configuration, Chem. Commun. (1997, 1969–1970.).
[25] M. Aguilar-Moncayo, T.M. Gloster, J.P. Turkenburg, M.I. García-Moreno, C. Ortiz Mellet, G.J. Davies, J. m., García Fernández. Glycosidase inhibition by ring-modified castanospermine analogues: Tackling enzyme selectivity by inhibitor tailoring, Org. Biomol. Chem. 7 (2009) 2738–2747.
[26] I.A. Bermejo, C.D. Navo, J. Castro-López, A. Guerreiro, E. Jiménez-Moreno, E. M. Sánchez-Fernández, F. Garcia-Martin, H. Hinou, S.I. Nishimura, J.M. García Fernández, C. Ortiz Mellet, A. Avenoza, J.H. Busto, G.J.L. Bernardes, R. Hurtado-Guerrero, J.M. Peregrina, J.M. Corzana, F. Synthesis, conformational analysis and in vivo assays of an anti-cancer vaccine that features an unnatural antigen based on an sp^2-iminosugar fragment, Chem. Sci. 11 (2020) 3996–4006.
[27] P.A. Guillén-Poza, E.M. Sánchez-Fernández, G. Artigas, J.M. García Fernández, H. Hinou, C. Ortiz Mellet, S.I. Nishimura, F. García-Martín, Amplified detection of breast cancer autoantibodies using MUC1-Based Tn antigen mimics, J. Med. Chem. 63 (2020) 8524–8533.
[28] M. González-Cuesta, I. Herrera-González, M.I. García-Moreno, R.A. Ashmus, D. J. Vocadlo, J.M. García Fernández, E. Nanba, K. Higaki, C., Ortiz Mellet. sp^2-Iminosugars targeting human lysosomal β-hexosaminidase as pharmacological chaperone candidates for late-onset Tay-Sachs disease, J. Enzyme Inhib. Med. Chem. 37 (2022) 1364–1374.
[29] M.C. Padilla-Pérez, E.M. Sánchez-Fernández, A. González-Bakker, A. Puerta, J. M. Padrón, F. Martín-Loro, A.I. Arroba, J.M. García Fernández, C. Ortiz Mellet, Fluoro-labelled sp^2-iminoglycolipids with immunomodulatory properties, Eur. J. Med. Chem. 255 (2023) 115390.
[30] M. González-Cuesta, A.-C.-Y. Lai, P.Y. Chi, I.-L. Hsu, N.-T. Liu, K.-C. Wu, J. M. García Fernández, Y.-J. Chang, C. Ortiz Mellet, Serine-/cysteine-based sp^2-iminoglycolipids as novel TLR4 agonists: Evaluation of their adjuvancy and immunotherapeutic properties in a murine model of asthma, J. Med. Chem. 66 (2023) 4768–4783.
[31] M. Aguilar-Moncayo, T. Takai, K. Higaki, T. Mena-Barragan, Y. Hirano, K. Yura, L. Li, Y. Yu, Y. Ninomiya, M.I. Garcia-Moreno, S. Ishii, Y. Sakakibara, K. Ohno, C. O. Nanba, J.M. Mellet, Y. Garcia Fernández, Suzuki., Tuning glycosidase inhibition through aglycone interactions: pharmacological chaperones for Fabry disease and GM1 gangliosidosis, Chem. Commun. 48 (2012) 6514–6516.
[32] T. Mena-Barragán, A. Narita, D. Matias, G. Tiscornia, E. Nanba, K. Ohno, Y. Suzui, K. Higaki, J.M. García Fernández, C. Ortiz Mellet, pH-Responsive pharmacological chaperones for rescuing mutant glycosidases, Angew. Chem. Int. Ed. Engl. 54 (2015) 11696–11700.
[33] R. Rísquez-Cuadro, R. Matsumoto, F. Ortega-Caballero, E. Nanba, K. Higaki, J. M. García Fernández, C. Ortiz Mellet, Pharmacological chaperones for the treatment of α-mannosidosis, J. Med. Chem. 62 (2019) 5832–5843.
[34] M. González-Cuesta, P. Sidhu, R.A. Ashmus, A. Males, C. Proceviat, Z. Madden, J. C. Rogalski, J.A. Busmann, L.J. Foster, J.M. García Fernández, G.J. Davies, C. Ortiz Mellet, D.J. Vocadlo, Bicyclic picomolar OGA inhibitors enable chemoproteomic

mapping of its endogenous post-translational modifications, J. Am. Chem. Soc. 144 (2022) 832–844.
[35] I.M. Welleman, M.W.H. Hoorens, B.L. Feringa, H.H. Boersma, W. Szymanski, Photoresponsive molecular tools for emerging applications of light in medicine, Chem. Sci. 11 (2020) 11672–11691.
[36] I. Herrera-González, M. González Cuesta, M.I. García Moreno, J.M. García Fernández, C. Ortiz Mellet, Stereoselective Synthesis of Nojirimycin α- C-Glycosides from a Bicyclic Acyliminium Intermediate: A Convenient Entry to *N*, C-Biantennary Glycomimetics, ACS Omega 7 (2022) 22394–22405.
[37] E.M. Sánchez-Fernández, R. García-Hernández, F. Gamarro, A.I. Arroba, M. Aguilar-Diosdado, J.M. Padrón, J.M. García Fernández, C. Ortiz Mellet, Synthesis of sp^2-Iminosugar Selenoglycolipids as Multitarget Drug Candidates with Antiproliferative, Leishmanicidal and Anti-Inflammatory Properties, Molecules 26 (2021) 7501.
[38] J. Kim, B.M. Novak, A.J. Waddon, Liquid Crystalline Properties of Polyguanidines *Macromolecules* 37 (2004) 8286–8292.
[39] S. Chen, C. Wang, Y. Yin, K. Chen, Synthesis of photo-responsive azobenzene molecules with different hydrophobic chain length for controlling foam stability, RSC Adv. 6 (2016) 60138–60144.
[40] E.M. Sánchez-Fernández, R. Rísquez-Cuadro, M. Chasseraud, A. Ahidouch, C. Ortiz Mellet, H. Ouadid-Ahidouch, J.M. García Fernández, Synthesis of *N*-, *S*-, and *C*-glycoside castanospermine analogues with selective neutral α-glucosidase inhibitory activity as antitumour agents, Chem. Commun. 46 (2010) 5328–5330.
[41] E.M. Sánchez-Fernández, R. Rísquez-Cuadro, C. Ortiz Mellet, J.M. García Fernández, P.M. Nieto, J. Angulo, sp^2-Iminosugar *O*-, *S*-, and *N*-Glycosides as conformational mimics of α-linked disaccharides; Implications for glycosidase inhibition, Chem. Eur. J. 18 (2012) 8527–8539.
[42] I. Herrera-González, M. Thépaut, E.M. Sánchez-Fernández, A. di Maio, C. Vivès, J. Rojo, J.M. García Fernández, F. Fieschi, P.M. Nieto, C. Ortiz Mellet, Mannobioside biomimetics that trigger DC-SIGN binding selectivity, Chem. Commun. 58 (2022) 12086–12089.
[43] I. Herrera-González, M. González-Cuesta, M. Thépaut, E. Laigre, D. Goyard, J. Rojo, J.M. García Fernández, F. Fieschi, O. Renaudet, P.M. Nieto, C. Ortiz Mellet, High Mannose Oligosaccharide Hemimimetics that Recapitulate the Conformation and Binding Mode to Concanavalin A, DC-SIGN and Langerin, Chem. Eur. J. (2023) e202303041.
[44] T. Fuchss, R.R. Schmidt, 5-Amino-5-deoxy-1-thioglucopyranosides-synthesis of thioglycoside derivatives of nojirimycin, J. Carbohydr. Chem. 19 (2000) 677–691.
[45] V.M. Díaz Pérez, M.I. García Moreno, C. Ortiz Mellet, J. Fuentes, J.C. Díaz Arribas, F. Cañada, J.M. García Fernández, Generalized Anomeric Effect in Action: Synthesis and evaluation of stable reducing indolizidine glycomimetics as glycosidase inhibitors, J. Org. Chem. 65 (2000) 136–143.
[46] G. Excoffier, D. Gagnaire, J.P. Utille, Coupure sélective par l'hydrazine des groupements acétyles anomères de résidus glycosyles acétylés, Carbohydr. Res. 39 (1975) 368–373.
[47] G. Wei, L. Zhang, C. Cai, S. Cheng, Y d., Selective cleavage of sugar anomeric *O*-acyl groups using $FeCl_3{\cdot}6H_2O$, Tetrahedron Lett. 49 (2008) 5488–5491.
[48] L. Baldini, D. Balestri, L. Marchiò, A. Casnati, A Combined Solution and Solid-State Study on the Tautomerism of an Azocalix[4]arene Chromoionophore, Molecules 28 (2023) 4704.
[49] C. Lin, S. Maisonneuve, C. Theulier, J. Xie, Synthesis and Photochromic Properties of Azobenzene-Derived Glycomacrolactones, Eur. J. Org. Chem. 1770–1777 (2019).
[50] Z. Wang, S. Maisonneuve, J. Xie, One-Pot Synthesis of Water-Soluble Glycosyl Azobenzenes and Their Photoswitching Properties in Water, J. Org. Chem. 87 (2022) 16165–16174.
[51] P. Díaz Pérez, M.I. García-Moreno, C. Ortiz Mellet, J.M. García Fernández, Synthesis and Comparative Glycosidase Inhibitory Properties of Reducing Castanospermine Analogues, Eur. J. Org. Chem. (2005) 2903–2913.
[52] E.M. Sánchez-Fernández, R. Rísquez-Cuadro, M. Aguilar-Moncayo, M.I. García-Moreno, C. Ortiz Mellet, J. m., García Fernández. Generalized Anomeric Effect in *gem*-Diamines: Stereoselective Synthesis of α-*N*-Linked Disaccharide Mimics, Org. Lett. 11 (2009) 3306–3309.
[53] E.M. Sánchez-Fernández, R. Gonçalves-Pereira, R. Rísquez-Cuadro, G.B. Plata, J. M. Padrón, J.M. García Fernández, C. Ortiz, Mellet, Carbohydr. Res. 429 (2016) 113–122.
[54] E. Drula, M.-L. Garron, S. Dogan, V. Lombard, B. Henrissat, N. Terrapon, The carbohydrate-active enzyme database: functions and literature, Nucleic Acids Res. 50 (2022) D571–D577.
[55] F.M. Platt, A. d'Azzo, B.L. Davidson, E.F. Neufeld, C.J. Tifft, Lysosomal storage diseases, Nat. Rev. Dis. Primers 4 (2018) 27.
[56] B. Brumshtein, M. Aguilar-Moncayo, M.I. García-Moreno, C. Ortiz Mellet, J. M. García Fernández, I. Silman, Y. Shaaltiel, D. Aviezer, J.L. Sussman, A. H. Futerman, 6-Amino-6-deoxy-5,6-di-N-(N′-octyliminomethylidene)nojirimycin: synthesis, biological evaluation, and crystal structure in complex with acid β-glucosidase, ChemBioChem 10 (2009) 1480–1485.
[57] J. Castilla, R. Rísquez, D. Cruz, K. Higaki, E. Nanba, K. Ohno, Y. Suzuki, Y. Díaz, C. Ortiz Mellet, J.M. García Fernández, S. Castillón, Conformationally-locked N-glycosides with selective β-glucosidase inhibitory activity: Identification of a new non-iminosugar-type pharmacological chaperone for gaucher disease, J. Med. Chem. 55 (2012) 6857–6865.
[58] F.M. Platt, Emptying the stores: lysosomal diseases and therapeutic strategies, Nat. Rev. Drug Discov. 17 (2018) 133–150.
[59] Y. Suzuki., Chaperone therapy for lysosomal and non-lysosomal protein misfolding diseases, Brain Dev. 45 (2023) 251–259.
[60] T. Mena-Barragán, M.I. García-Moreno, A. Sevšek, T. Okazaki, E. Nanba, K. Higaki, N.I. Martin, R.J. Pieters, J.M. García Fernández, C. Ortiz Mellet, Probing the Inhibitor versus Chaperone Properties of sp^2-Iminosugars towards Human β-Glucocerebrosidase: A Picomolar Chaperone for Gaucher Disease, Molecules 23 (2018) 927.